Photoemission study of composition- and temperature-induced metal-insulator transitions in Cr-doped V_2O_3

Kevin E. Smith
Department of Physics, Boston University, Boston, Massachusetts 02215

Victor E. Henrich
Department of Applied Physics, Yale University, New Haven, Connecticut 06520
(Received 30 November 1993; revised manuscript received 16 March 1994)

The variety and complexity of the metal-insulator transitions that V_2O_3 undergoes, in both pure form and when doped with other transition-metal ions, have resulted in widespread interest in the electronic structure of this oxide. We report here the results of a photoemission study of the electronic structure of Cr-doped V_2O_3 in metallic and insulating states. At room temperature, insulating Cr-doped V_2O_3 exhibits a low emission intensity at E_F. When cooled, a transition to a metallic state is observed at 210 K. The emission intensity at E_F and the width of the V $3d$ emission increase below this transition. Additionally, the O $1s$ and V $2p$ core-level structure changes, resembling that of the metallic state of pure V_2O_3. When cooled further, another transition occurs from the metallic state to a second insulating state. The emission intensity at E_F decreases and the V $3d$ emission narrows. The core-level emission structure reverted to that of the room-temperature insulating state. The changes in density-of-states and bandwidth were found to be consistent with a Fermi-liquid theory of these transitions; the changes in core-level emission are identified with different core-hole screening in the metallic and insulating states.

I. INTRODUCTION

The variety and complexity of the metal-insulator transitions which V_2O_3 undergoes, in both pure form and when doped with other transition-metal ions, have resulted in widespread interest in the electronic structure of these oxides. Pure V_2O_3 goes through two metal-insulator transitions as a function of temperature: a first-order transition at 150 K from a monoclinic antiferromagnetic insulator at low temperatures to a trigonal metallic state, and a broad ($\approx$150 K) second-order transition from this metallic state to a semiconducting one at 450–500 K.[1] When doped with Cr, additional transitions occur. First, the metallic state becomes progressively more insulating at a fixed temperature with the addition of Cr, the resistivity rising by an order of magnitude for each atomic % Cr incorporated into the crystal.[2] Second, a transition is observed as the temperature is increased above 170 K;[2,3] the trigonal metallic state is observed to revert to an insulating state, but with no change in crystal symmetry. The temperature at which this transition occurs is a function of the Cr concentration. (This transition from the metallic to the insulating state with increasing temperature will be referred to here as the high-temperature transition; the transition from an antiferromagnetic insulator to a metallic state at approximately 150–170 K, which also occurs in pure V_2O_3, is referred to here as the low-temperature transition.) These transitions are clearly visible in the resistivity versus temperature plot of Kuwamoto, Honig, and Appel,[2] which is reproduced in Fig. 1. The nature of these transitions has been the subject of numerous studies (see Refs. 1, 2, 4–8, and references therein).

Many experimental techniques have been used to study the nature of the metal-insulator transitions in Cr-doped V_2O_3.[2] However, despite the fact that photoemission spectroscopy is a powerful tool for determining electronic structure in solids, it has not been widely applied to these oxides. The goals of the study reported here were to use

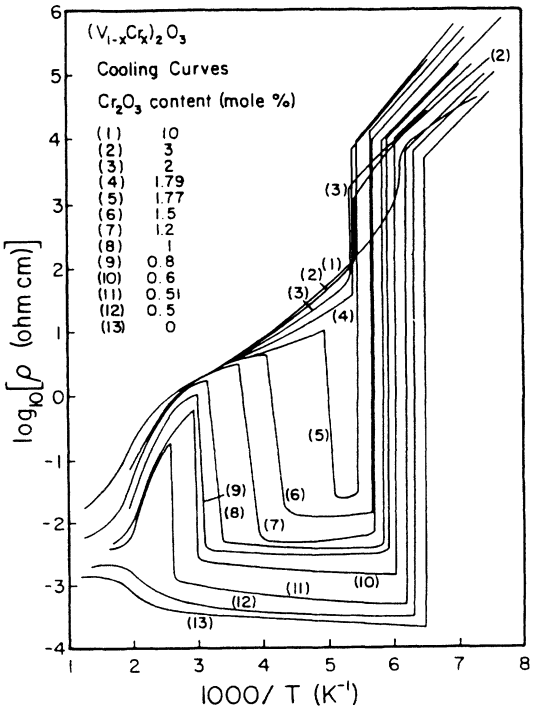

FIG. 1. Variation of resistivity with temperature for Cr-doped V_2O_3. (From Ref. 2.)

photoemission spectroscopy to measure electronic structure in the Cr-V_2O_3 system, as a function of temperature and Cr content. We report the first observation using photoemission of metal-insulator transitions in single-crystal Cr-doped V_2O_3 cleaved in UHV. Dramatic changes in the density-of-states at the Fermi level (E_F) are observed as both the low- and high-temperature transitions are crossed, and as the Cr content is varied. The effect of screening on the core-level spectra is revealed by examining the V $2p$ core levels in both metallic and insulating phases; the origin of a previously observed[9,10] doublet structure of the V $2p_{3/2}$ and V $2p_{1/2}$ lines is assigned to well-screened and poorly-screened emission.

II. PURE AND CR-DOPED V_2O_3: BULK AND SURFACE PROPERTIES

V_2O_3 has the corundum structure with a trigonal (rhombohedral) Bravais lattice. When doped with Cr, V_2O_3 retains the corundum structure at room temperature, with the Cr entering the lattice substitutionally.[1] The unit cell consists of a ten-atom basis made up of two M_2O_3 molecular units. The crystal field splits the atomic d states into a pair of e_g^σ orbitals, a pair of e_g^π orbitals, and an a_{1g} orbital.[1] The room-temperature metallic phase in V_2O_3 displays a variety of anomalous properties, among them an extremely large T^2 term in the electrical resistivity (10^3 times larger than in transition metals),[11] and a very large electronic specific heat.[12] Central to understanding V_2O_3 is the realization that it possesses two types of $3d$ electrons; with a $3d^2$ configuration, both the a_{1g} and e_g^π bands are partially populated. The order of these bands in energy was originally determined from optical experiments.[13] The most comprehensive theory of the metallic states assumes a Hubbard model and has the a_{1g} orbital half full, with 0.5 electrons per V atom contained within it and the remaining 1.5 electrons per V atom residing in the e_g^π band.[14] E_F lies within both bands, but the thermodynamic and transport properties of metallic V_2O_3 are postulated to be determined primarily by the e_g^π electrons. The electronic structure for single crystals of pure V_2O_3 has been studied by a number of groups using photoemission spectroscopy.[15–18] The reader is referred to Refs. 15 and 16 for discussion of band dispersion and hybridization in this system.

V_2O_3 single crystals cleave to expose the $(10\bar{1}2)$ surface. The electronic structure of nearly perfect $V_2O_3(10\bar{1}2)$ surfaces has been previously shown by photoemission to have the same general structure as the bulk, and the ion bombardment was found to remove oxygen from $V_2O_3(10\bar{1}2)$, reducing the surface.[9] In general, the adsorption properties of $V_2O_3(10\bar{1}2)$ are similar to those of the related compound $Ti_2O_3(10\bar{1}2)$.[19,20]

III. EXPERIMENTAL METHOD

The experimental apparatus and sample preparation techniques are briefly described here; a detailed discussion of the former topic can be found elsewhere.[5,21–23] Ultraviolet photoemission spectroscopy (UPS) using both resonance lamps and synchrotron radiation, and x-ray-photoemission spectroscopy (XPS) using an x-ray anode source were used in this study. He I photons at 21.2 eV were obtained from a He microwave discharge lamp, and spectra presented here were corrected for impurity lines in the lamp. X-ray photons were obtained from an Al anode x-ray source. Unless otherwise stated, spectra were recorded with the sample held at room temperature. E_F was determined from an atomically clean gold foil in contact with the sample, and all binding energies are referenced to the Au $4f_{7/2}$ peak at 84.0 eV. All spectra were recorded in an angle-integrated mode, using a double-pass cylindrical mirror analyzer (CMA) to measure electron kinetic energies; the overall energy resolution for UPS spectra was 250 meV and for XPS was 800 meV. Experiments using synchrotron radiation were performed on beamline U14A at the National Synchrotron Light Source, Brookhaven National Laboratory. Angle-integrated spectra were taken using a CMA. Spectra were taken with the photon beam incident at approximately 60° off the sample normal and the CMA axis at 45°.

Nearly perfect $(10\bar{1}2)$ surfaces of pure and Cr-doped V_2O_3 (1.5 and 3 at. %) were prepared by cleaving in pressures $<2\times10^{-10}$ Torr. The crystals were oriented using Laue x-ray diffraction and cut into rods approximately $3\times3\times10$ mm^3, with the long axis perpendicular to the $(10\bar{1}2)$ plane. Shallow grooves were cut every 1 mm on the side of the rods to facilitate cleavage. High-defect-density V_2O_3 surfaces were prepared by Ar^+ ion bombardment of the cleaved surface. Ion bombardment was performed with the chamber pressure at 5×10^{-5} Torr of Ar. Samples could be heated to above 900 K and cooled to approximately 125 K by using a combined resistance heated/liquid nitrogen cooled sample holder.

IV. RESULTS

A. Pure and Cr-doped V_2O_3 at 300 K

Figure 1 shows the temperature and Cr concentration dependence of the resistivity of Cr-doped V_2O_3 single crystals. It is clear from this figure that both the 1.5 and 3 at. % Cr samples should be insulating at room temperature, with resistivities three to four orders of magnitude larger than that of pure V_2O_3, which is metallic at this temperature. Thus the incorporation of Cr into the lattice induces a metal-insulator transition at room temperature in V_2O_3. Figure 2 shows the UPS spectra obtained from both pure and Cr-doped V_2O_3 $(10\bar{1}2)$ (3 at. % Cr) single-crystal surfaces using synchrotron radiation ($h\nu=44$ eV). The spectra of Fig. 2 are normalized to have the same O $2p$ emission intensity (area). A dramatic shift of the V $3d$ emission away from E_F is visible in Fig. 2 for the Cr-doped V_2O_3; E_F lies within the V $3d$ band in pure, metallic V_2O_3, and consequently the spectrum from V_2O_3 exhibits significant emission at E_F. However, the intensity at E_F for the Cr-doped sample is much smaller. Thus the opening of a gap, or a very large decrease in the electron density at E_F, is clearly visible in the spectra from room temperature V_2O_3 doped with 3 at. % Cr when compared with pure V_2O_3. The relative V $(3d)$/O

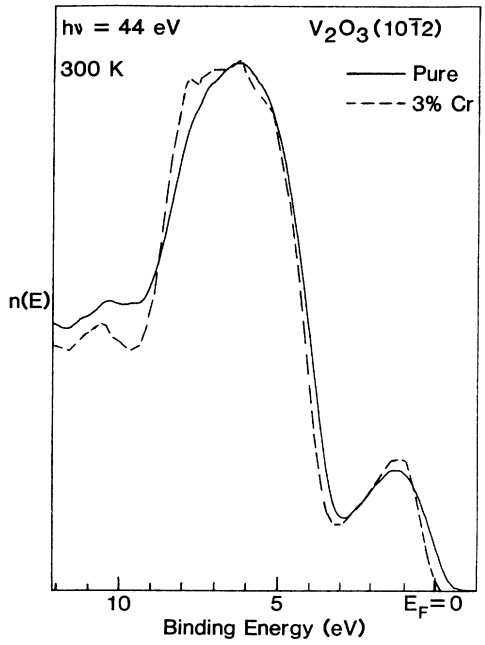

FIG. 2. Room temperature UPS spectra for pure and 3% Cr-doped $V_2O_3(10\bar{1}2)$. ($h\nu$=44 eV.)

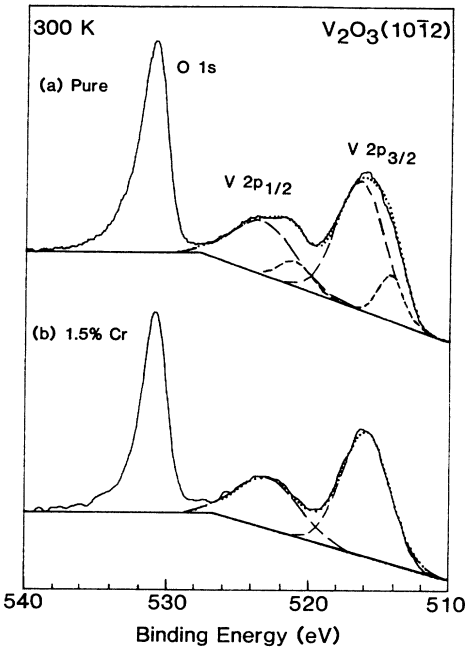

FIG. 3. O 1s and V 2p spectra from room temperature ($10\bar{1}2$) surfaces. (a) pure V_2O_3 (from Ref. 4); (b) V_2O_3 doped with 1.5% Cr. ($h\nu$=1486.6 eV.)

(2p) intensity ratio is 0.11 in pure V_2O_3 and 0.12 in Cr-doped V_2O_3 (Fig. 2), although this small a difference in intensity may not be significant. The addition of Cr into V_2O_3 also results in a shift of the O 2p emission away from E_F, but by a smaller amount than for the V 3d emission; the top of the O 2p band shifts to higher binding energy by 0.15 eV. As described elsewhere, the photon energy dependence of the V 3d and O 2p emission intensity from Cr-doped V_2O_3 is very similar to that from pure V_2O_3.[16]

Figure 3(a) shows the O 1s and V 2p core-level XPS spectra from room-temperature cleaved Cr-doped $V_2O_3(10\bar{1}2)$ (1.5% Cr); Fig. 3(b) shows the equivalent spectra from pure V_2O_3 as determined previously.[9,10] The V 2p emission is multiplet split into V $2p_{1/2}$ and V $2p_{3/2}$ peaks. For illustrative purposes only, the V 2p peaks were deconvoluted into the minimum number of Gaussians which would adequately fit the spectra (above the straight line background shown in Fig. 3). For pure V_2O_3, it was found that the V $2p_{1/2}$, $2p_{3/2}$ emission features could only be satisfactorily deconvoluted by *two* pairs of Gaussians.[9] These were constrained to have the same peak separation (6.9 eV) and approximately the same relative intensity and full width at half maximum (FWHM). The pairs were then shifted rigidly in binding energy until the best fit was obtained; the resultant shift was 2.2 eV. These parameters are listed in Table I. The binding energies of the major V $2p_{3/2}$ and V $2p_{1/2}$ Gaussians were found to be 516.5 and 523.4 eV, respectively.[9]

The V 2p emission from room-temperature cleaved Cr-doped V_2O_3 (1.5% Cr), however, can be satisfactorily reproduced by using only *one* pair of Gaussian peaks; this is shown in Fig. 3(a). These Gaussians are almost identical to the major pair of Gaussians used in the pure V_2O_3 deconvolution (the relative intensity ratio is slightly larger), but they are shifted to lower binding energy by 0.6 eV. The parameters for these peaks are listed in Table I. Thus, the minor pair of peaks required to model the V 2p emission from pure V_2O_3 (at 2.2 eV lower binding energy than the major pair) are not required in the case of Cr-doped V_2O_3 at room temperature. Note also that there exists an asymmetry on the high-binding-energy side of the O 1s emission from pure V_2O_3 [Fig. 3(b)]; this asymmetry is significantly reduced in the O 1s emission from Cr-doped V_2O_3. The binding energy of the O 1s emission in both pure[9] and Cr-doped V_2O_3 is 530.9 eV. The origins of the significant charges in line shape of both cation and anion core-level emission from V_2O_3 when doped with Cr will be discussed below.

B. Cr-doped V_2O_3 at < 300 K

The resistivity vs temperature plot of Fig. 1 indicates that a V_2O_3 crystal doped with 1.5 at. % Cr should be insulating at room temperature and have nearly the same resistivity as one doped with 3% Cr. The UPS spectra from both 1.5 and 3% Cr-doped samples were found to be essentially identical at room temperature; the 3% Cr spectrum is shown in Fig. 2. As the V_2O_3 crystal doped with 1.5% Cr is cooled below room temperature, it experiences two metal-insulator transitions (Fig. 1). At approximately 240 K the resistivity drops by almost three orders of magnitude and the sample becomes metallic; note, however, that the resistivity in this state is still almost two orders of magnitude larger than that of the metallic state in pure V_2O_3. Further cooling of the crystal

TABLE I. Parameters for Gaussians used to fit the V 2*p* emission features in Fig. 3. WS = well screened, PS = poorly screened.

Material	Binding energy (eV)	Origin	FWHM (eV)	Relative area
V_2O_3 at 300 K	516.5	V $2p_{3/2}$ PS	4.1	1
(Refs. 9 and 10)	523.4	V $2p_{1/2}$ PS	5.2	0.53
	514.3	V $2p_{3/2}$ WS	2.2	1
	521.2	V $2p_{1/2}$ WS	2.6	0.64
Cr-doped V_2O_3	515.9	V $2p_{3/2}$ PS	4.1	1
(1.5% Cr) at 300 K	522.8	V $2p_{1/2}$ PS	5.2	0.41

causes the resistivity to rise again; at approximately 170 K the sample returns to an insulating state, with a six order-of-magnitude change in resistivity from the metallic state. Note here that the resistivity of this low-temperature insulating state is more than a thousand times larger than that of the room-temperature insulating state.

Figure 4 presents the UPS spectra obtained from a cleaved $(10\bar{1}2)$ surface of V_2O_3 doped with 1.5% Cr as the crystal is cooled below room temperature. The spectrum taken with the crystal at 240 K is similar to the room-temperature spectrum, with a very low density of electrons visible at E_F. Upon cooling the sample to 210 K, the UPS spectrum changes dramatically, with the V 3*d* states shifting towards E_F. Further cooling to 180 K does not result in any significant change in the UPS spectrum. However, when the crystal is cooled to 130 K, the UPS spectrum again changes dramatically: the V 3*d* emission moves away from E_F and a gap in the emission is seen to open up at E_F. Thus, as the crystal is taken through the two metal-insulator transitions described

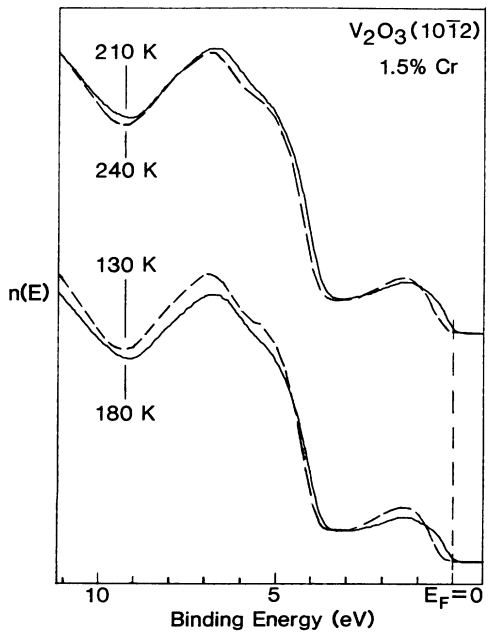

FIG. 4. UPS spectra from cleaved 1.5% Cr-doped V_2O_3 $(10\bar{1}2)$ cooled to 240, 210, 180, and 130 K. ($h\nu$=21.2 eV.)

above, large changes in the density of states at E_F are observed. This is the first unambiguous valence-band photoemission observation of the high- and low-temperature metal-insulator transitions in Cr-doped V_2O_3.

The intensity of the V 3*d* emission changes only slightly as the crystal undergoes these metal-insulator transitions. The integrated area of the V 3*d* emission above a linear background decreases 6% in going from the room-temperature insulating state to the metallic state at 210 K. Upon going from the metallic state to the low-temperature insulating state, the V 3*d* emission increases in intensity by 3%. However, these changes are small enough that they may not be significant. Additionally, the O 2*p* band is observed to shift during the metal-insulator transitions. At the high-temperature transition, the top of the O 2*p* band moves towards E_F by approximately 0.1 eV as the material becomes metallic. At the low-temperature transition, the O 2*p* band moves away from E_F by the same amount as the material reverts to an insulating state.

The O 1*s* and V 2*p* XPS spectra for this sample in both the insulating phase at 240 K and the metallic phase at 180 K are shown in Figs. 5(a) and 5(b), respectively. The 240 K spectrum is very similar to that obtained in the low-temperature insulating phase at 130 K, and consequently the latter spectrum is not shown. The spectrum obtained from the 240-K-insulating sample is also very similar to the room-temperature spectrum of Fig. 3(a). As in that case, the V 2*p* spectrum can be reproduced by using only *one* pair of Gaussians. The separation of these Gaussians and their FWHM and relative intensities are identical to the Gaussians required to fit the room-temperature spectrum; these parameters are listed in Table II. Note that the binding energies of these Gaussians are 0.1 eV lower for the 240-K spectrum than for the room-temperature spectrum. When the crystal goes through the high-temperature transition and becomes metallic, the V 2*p* core-level spectra change dramatically. The O 1*s* and V 2*p* spectra from a crystal at 180 K are shown in Fig. 5(b). It is clear in this figure that *two* pairs of Gaussians are now required to adequately fit the spectrum. The parameters for these Gaussians are also listed in Table II. These parameters are, with the exception of the absolute binding energies, remarkably similar to those of pure, metallic, V_2O_3 (see Table I); there is, however, an increase in the separation of the two pairs of Gaussians of 0.2 eV, from 2.2 eV for pure V_2O_3 to 2.4 eV for V_2O_3

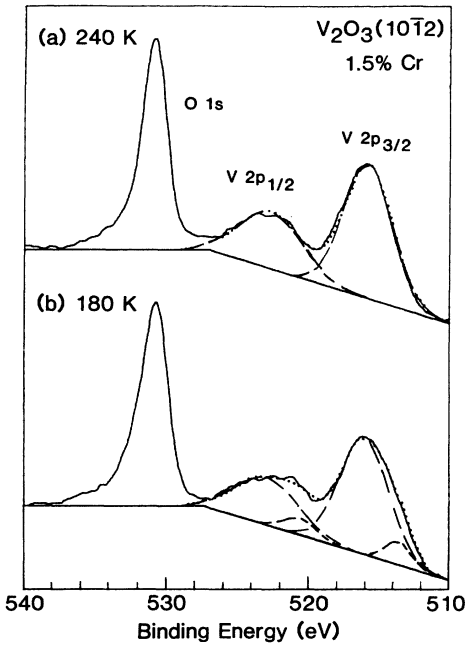

FIG. 5. O 1*s* and V 2*p* XPS spectra from cleaved 1.5% Cr-doped $V_2O_3(10\bar{1}2)$ surfaces at (a) 240 K, and (b) 180 K. ($h\nu$=1486.6 eV.)

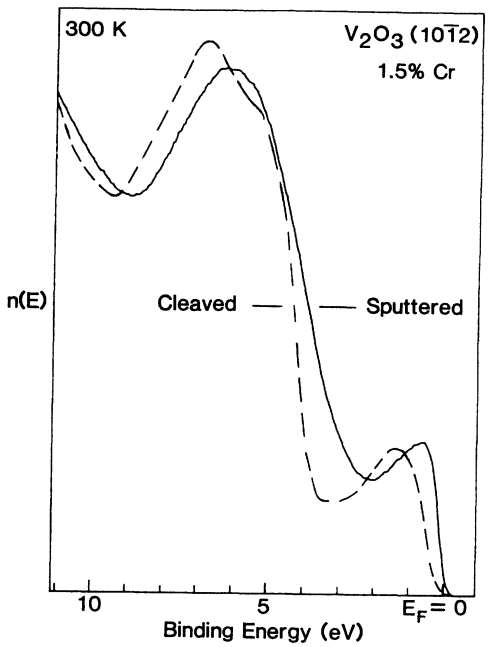

FIG. 6. UPS spectra from cleaved and sputtered 1.5% Cr-doped $V_2O_3(10\bar{1}2)$ at room temperature. ($h\nu$=21.2 eV.)

doped with 1.5% Cr at 180 K. As mentioned above, further cooling the sample to 130 K results in an O 1*s*/V 2*p* spectrum very similar to the 240-K spectrum of Fig. 5(a). Thus, in both the low- and high-temperature insulating phases, only one pair of Gaussians is required to fit the V 2*p* spectrum, while two pairs are required in the metallic phase (as for pure V_2O_3). Note also that the O 1*s* line in Fig. 5 becomes more asymmetrical in the metallic phase. The origins of these changes will be discussed in Sec. V.

C. Cr-doped V_2O_3 ($10\bar{1}2$): Defect properties

The work function, Φ, of a surface can be determined via photoemission by measuring the vacuum level cutoff in the UPS spectrum. Using this method, Φ for room-temperature insulating V_2O_3 ($10\bar{1}2$) doped with 1.5% Cr was determined to be 4.2 eV. This contrasts sharply with the value of 4.9 eV obtained for pure $V_2O_3(10\bar{1}2)$.[9] When the Cr-doped V_2O_3 becomes metallic at 210 K, no change in Φ is observed. Preliminary results indicate that the interaction of O_2 with cleaved Cr-doped $V_2O_3(10\bar{1}2)$ (1.5% Cr) at room temperature is similar to that on pure V_2O_3. Ar^+-ion bombardment of the cleaved Cr-doped $V_2O_3(10\bar{1}2)$ surface (1.5% Cr) results in the preferential removal of oxygen anions and consequent reduction of the surface. Figure 6 shows the UPS spectra from cleaved $V_2O_3(10\bar{1}2)$ doped with 1.5% Cr at room temperature, and that surface sputtered for 30 min with 1-keV-Ar^+ ions. The cleaved surface is insulating at room temperature, as discussed above, and has a low density of electrons at E_F. The sputtered surface, in contrast, shows a very high density of electrons at E_F, consistent with the metallic nature of the reduced surface. The work function of the sputtered surface is 4.4 eV, 0.2 eV higher than that of the cleaved surface. Figure 7 shows the changes in the O 1*s* and V 2*p* core-level structure induced by sputtering. The O 1*s* line broadens but the binding energy remains unchanged. The V 2*p* emission becomes asymmetrical and shifts to lower binding energy.

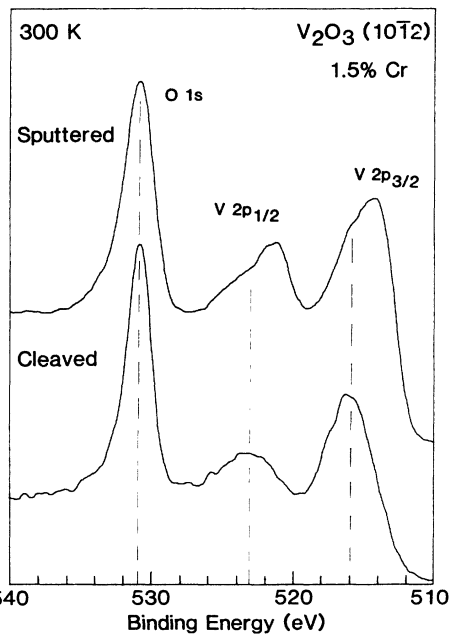

FIG. 7. O 1*s* and V 2*p* XPS spectra from cleaved and sputtered 1.5% Cr-doped $V_2O_3(10\bar{1}2)$ at room temperature. ($h\nu$=1486.6 eV.)

TABLE II. Parameters for Gaussians used to fit the V $2p$ emission features in Fig. 5. WS = well screened, PS = poorly screened.

Material	Binding energy (eV)	Origin	FWHM (eV)	Relative area
Cr-doped V_2O_3 (1.5% Cr) at 240 K)	515.8	V $2p_{3/2}$ PS	4.1	1
Cr-doped V_2O_3 (1.5% Cr) at 180 K	516.0	V $2p_{3/2}$ PS	4.1	1
	522.9	V $2p_{1/2}$ PS	5.2	0.41
	513.6	V $2p_{3/2}$ WS	2.2	1
	520.5	V $2p_{1/2}$ WS	2.6	0.8

Kurtz[9,10] has fit the V $2p$ spectrum from sputtered V_2O_3 with six Gaussians. The relative O $1s$-V $2p$ energy separation of the emission from sputtered Cr-doped V_2O_3 (Fig. 7) is identical to that from sputtered pure V_2O_3.[9,10]

V. DISCUSSION

The data presented in the previous section comprise the first unambiguous ultraviolet and x-ray-photoemission observation of both composition and temperature-induced metal-insulator transitions in Cr-doped V_2O_3. One previous photoemission investigation of changes close to E_F during these transitions has been published,[24] but the surfaces used in that study were severely oxidized; a discussion of the previously published spectra will be presented later. First, each of the metal-insulator transitions observed in this study will be discussed below in the context of relevant theories.

The mechanisms underlying these transitions are the subject of much controversy,[2] but all are related (to a greater or lesser extent) to the concept of a Mott insulator.[25] A review of this concept is presented in Ref. 25; here, it is useful to restate the most relevant features of the theory. Mott's hypothesis is that a crystalline array of hydrogenlike atoms does not necessarily show metallic conduction, and that as the lattice parameter of the array is decreased there will be a sharp transition from an insulating to a metallic state.[6,25] The origin of this effect lies in the long-range part of the Coulomb force, which creates electron-hole bound states unless there is a sufficient density of electrons to screen the core potential.[6] Hubbard introduced U/W as the relevant parameter for the problem, where U is the intra-atomic Coulomb energy and W is the one-electron bandwidth.[26] Typically, when $U/W<1$ a rigid-band picture is a valid description of the electronic structure, whereas if $U/W>1$ a highly correlated electron-gas picture is usually more valid;[9] in V_2O_3, $U/W\approx 1$. A variety of physical mechanisms has been proposed to explain the transitions in Cr-doped V_2O_3, particularly the high-temperature transition, and many rely on the Mott-Hubbard concept. A thermodynamic theory by Spalek, Datta, and Honig[27] based on Fermi-liquid theory, and consisting of bands narrowed by correlations transforming into a lattice of localized spins, predicts many of the features of the Cr-doped V_2O_3 phase diagram.

A. Composition-induced transition

The UPS spectra of Fig. 2 indicate that as Cr is added to V_3O_3, the material goes from a room-temperature metallic state to an insulating one. A band gap opens up in the cation $3d$ band, with a very low density of electrons detected at E_F in the Cr-doped samples. This is consistent with the bulk resistivity data of Fig. 1. In the theory of Spalek, Datta, and Honig,[27] the effective Hubbard parameter U/W increases linearly with Cr content, with both an increase in U and a decrease in W. At the critical value of $U/W=1.646$, a discontinuous transition from a metallic to an insulating phase is predicted. The UPS spectra of Fig. 2 indicate that, as Cr is added to V_2O_3, the V $3d$ emission not only moves away from E_F, but narrows as well. The width of the V $3d$ emission above a straight-line background decreases by approximately 0.3 eV when the spectrum from pure V_2O_3 is compared with one from a crystal doped with 3% Cr. This direct observation of a narrowing in the V $3d$ density of states is consistent with the model described above. The dramatic changes in the core-level spectra of Fig. 3 during this composition-induced transition will be discussed below, together with the similar changes observed during the temperature-induced transition (Fig. 5).

B. Temperature-induced transitions

The photoemission spectra of Fig. 4 reveal sharp changes in the density of states at E_F when a V_2O_3 crystal doped with 1.5% Cr is taken through both the high- and low-temperature transitions. As the sample is cooled from room temperature to 210 K it becomes metallic (with no change in lattice symmetry), with the V $3d$ emission observed to shift towards E_F (Fig. 2). Note, however, that the metallic phase exhibits a smaller density of electrons at E_F than does pure V_2O_3 at room temperature (Fig. 2). This is consistent with the observation that the resistivity in the metallic phase of 1.5% Cr-doped V_2O_3 is almost one-hundred times that of pure metallic V_2O_3 (Fig. 1), and the assertion by Kuwamoto, Honig, and Appel[2] that even in the metallic phase the density of elec-

trons at E_F must be extremely low. The origins of this high-temperature first-order transition are quite complex and are the subject of much controversy; eight distinct mechanisms are listed in Ref. 2. However, the theory of Spalek, Datta, and Honig[27] discussed above predicts the three metal-insulator transitions in Cr-doped V_2O_3 (the composition-induced and the high- and low-temperature transitions). A common feature of many of these theories is a narrowing of the V 3*d* bands in the insulating phase. Analysis of the data in Fig. 4 reveals that the V 3*d* emission in the room-temperature insulating state is 0.15 eV narrower than that in the metallic state at 210 K. This observation is consistent with the above theories, and the fact that the V 3*d* emission is consequently 0.15 eV narrower in the metallic state of Cr-doped V_2O_3 than the metallic state of pure V_2O_3 is consistent with the higher resistivity of the 210 K Cr-doped V_2O_3 metallic state.

When cooled further to 130 K, the spectra of Fig. 4 show that the material reverts to an insulating state. The UPS spectra reveal that the density of states at E_F is considerably smaller at 130 K than at 180 K. As with the high-temperature transition, the V 3*d* emission narrows as the material becomes more insulating. The symmetry of the lattice changes during this transition, going from trigonal in the metallic to monoclinic in the insulating state.[1] Additionally, the volume increases by up to 3.5% at the low-temperature transition.[1] The mechanism driving this transition (which also occurs in pure V_2O_3) is somewhat different from that driving the high-temperature transition although the previously mentioned theory of Spalek, Datta, and Honig[27] predicts both. Specifically, low-temperature transition is driven by the Coulomb interaction between vanadium *d* electrons, which results in an antiferromagnetic arrangement of relatively localized spins.[2] (The low-temperature insulating phase is antiferromagnetic, while the metallic phase is paramagnetic.) However, the observed narrowing of the V 3*d* emission and opening up of a gap at E_F are consistent with theory.[2,27]

C. Core-level structure

Dramatic changes occur in the V $2p_{1/2}$ and V $2p_{3/2}$ core-level spectra when either the composition- (Fig. 3) or temperature-induced (Fig. 5) transitions are encountered. As described above, when Cr-doped V_2O_3 is in an insulating state, either at room temperature or at 130 K, the V 2*p* doublet is adequately described by a single pair of Gaussian peaks. This is in sharp contrast to the situation in metallic V_2O_3 at room temperature, or metallic Cr-doped V_2O_3 at 210 K, where two pairs of Gaussian peaks are required to fit the V 2*p* doublet. The parameters for these Gaussians are presented in Tables I and II. The origin of these extra peaks in pure V_2O_3 is a matter of some dispute. They are seen only in single-crystal samples cleaved in UHV;[9,10] V_2O_3 samples prepared in other fashions do not show this structure.[28] The possibility that these peaks are due to screening effects of the core holes has been proposed previously as the most likely origin.[9] The data presented here show conclusively that this is indeed the case and that these extra peaks in the metallic phase are due to the different response of the electrons in Cr-doped V_2O_3 to the production of cation core holes when the material is insulating or metallic. These changes in the V 2*p* core-level structure are not related to chemical shifts of the V 2*p* level as the material undergoes a metallic-insulator transition, but rather are related to the photoemission process itself (the 0.6-eV shift in the binding energy of the major Gaussian peaks between pure and Cr-doped V_2O_3 listed in Table I is, however, likely to be a chemical shift). The ability to turn on and off metallic screening by taking this material through a metal-insulator transition allows unambiguous identification of the effects of such screening.

A variety of screening phenomena can occur in transition-metal oxides during photoemission. Even in the absence of a significant electron density near E_F, core holes are to some extent screened by the electrons in the solid.[29–31] Thus when Cr-doped V_2O_3 is insulating at room temperature and has few electrons at E_F, the resulting V 2*p* binding energies are characteristic of poorly-screened emission rather than unscreened emission. When the crystal becomes metallic at 210 K, there are many more electrons at E_F with which to screen the core hole, and metallic screening occurs. Thus, the small pair of Gaussians which are seen in the deconvolution of the V 2*p* doublet in the metallic state are associated with well-screened emission from the V 2*p* levels and the large pair with the poorly-screened emission. Note that the valence-band satellite seen in V_2O_3 below the O 2*p* emission has a somewhat different origin than these well-screened peaks.[15,16]

The O 1*s* emission also changes shape as a metal-insulator transition occurs. In metallic V_2O_3 and Cr-doped V_2O_3 the O 1*s* line has a large asymmetry on the high-binding-energy side of the peak (Figs. 3 and 5). This is explained as arising from the production of electron-hole pairs at E_F as the high-energy photoemitted electrons leave the crystal.[9,10] Creation of these electron-hole pairs reduces the energy of the photoemitted O 1*s* electrons, and they consequently appear to have higher binding energies. This asymmetrical line shape is known as a Doniach-Sunjic line shape.[32] If this is indeed the origin of the asymmetry, then when the material becomes insulating and the density of electrons at E_F falls, this asymmetry should be significantly reduced. This is precisely what is observed in the insulating samples (Figs. 3 and 5), thus conclusively identifying the origin of this asymmetry.

D. Comparison with published data

Prior to this study, two photoemission investigations of metal-insulator transitions in Cr-doped V_2O_3 single crystals have been published.[24,33] Only Ref. 24 presents valence-band UPS spectra, and these spectra are inconclusive and contradict the results presented here. The spectra in Ref. 24 show a very small V 3*d* emission feature near E_F. This would imply that the surfaces are heavily oxidized. [It is not stated in Ref. 24 how the surfaces were prepared, but it is stated that they were cleaned until a reproducible O 1*s* line shape was obtained.

If the materials were cleaned by sputtering, a reduction of the surface would occur (Fig. 6), and the V 3*d* emission would be very large. Thus it appears their surfaces may have been annealed, which typically oxidizes the surface.] The UPS spectra in Ref. 24 do not show any significant changes during the metal-insulator transitions. Valence-band XPS spectra were also taken, and these seem to show effects similar to those seen in UPS spectra here for the V 3*d* emission during the transitions. However, the resolution of these XPS spectra is poor and the observed shifts are small.[24]

The second study, by Shin *et al.*,[33] examined the effect of the metal-insulator transition in pure and Cr-doped V_2O_3 on the V 3*p* and 3*s* emission. The authors do not present any valence-band spectra in this paper, but do observe changes in the V 3*s* emission as the samples are cooled. These were used to extract information on local magnetic moments, but provide no information on the structure close to E_F. It is not clear in this paper how the surfaces were prepared. (This paper erroneously states that Refs. 15 and 16 reported no change in the valence-band emission close to E_F in V_2O_3 when cooled through the metal-insulator transition; the experiments in Refs. 15 and 16 were performed at room temperature.)

The low-temperature transition in pure V_2O_3 powders has been observed using both UPS[34–36] and XPS.[28,35–37] The various surface preparations used in some of these studies make the data ambiguous. However, in both the work of Beatham and co-workers[34,35] and Sawatzky and Post,[28] changes in the density states at E_F were clearly observed when pure V_2O_3 was cooled through the low-temperature metal-antiferromagnetic insulator transition. Surprisingly, Shin *et al.*[18] report no change in the UPS spectra of scraped single-crystal V_2O_3 when cooled through this transition.

The metal-insulator transition in VO_2 powders[34,38,39] and small single crystals[40] has also been studied using photoemission. VO_2 undergoes a metal-insulator transition at 340 K,[1] and UPS spectra obtained from single-crystal samples by Bermudez *et al.*[40] clearly show significant changes in the valence-band structure as the material switches from an insulator at room temperature to a metal at 340 K. The metal-insulator transition is also visible in the XPS spectra obtained of powdered VO_2.[38] The V 2*p* doublet exhibits changes similar to those seen here, but the authors do not attempt to explain the line shape in terms of core-hole screening.[38]

VI. CONCLUSIONS

The electronic structure of Cr-doped V_2O_3 in metallic and insulating states has been investigated using both UPS and XPS. Addition of Cr to V_2O_3 was seen to produce insulating samples at room temperature, with a low density of electrons at E_F as indicated by the UPS results. Pronounced changes in the core-level emission were also observed when V_2O_3 was doped with Cr. Insulating Cr-doped V_2O_3 was cooled and a transition to a metallic state observed at 210 K. The density of electrons at E_F was seen to rise and the width of the V 3*d* emission increases following this transition. Additionally, the O 1*s* and V 2*p* core-level structure changed, resembling the metallic state of pure V_2O_3. As the crystal was cooled further, a second transition occurred from the metallic state to another insulating state. Again the density of electrons at E_F was observed to fall and the V 3*d* emission narrow. The core-level emission structure reverts to that of the room-temperature insulating state. The changes in density of states and bandwidth were found to be consistent with a Fermi-liquid theory of these transitions; the changes in core-level emission were identified with different photoemission-related processes (core-hole screening) in the metallic and insulating states.

ACKNOWLEDGMENTS

The authors acknowledge partial support of this work by NSF Solid State Chemistry Grants DMR 87-11423 and DMR 90-15488. K.E.S. also acknowledges the donors of the Petroleum Research Fund, administered by the American Chemical Society for partial support of this work. Some of the research was undertaken at the National Synchrotron Light Source, Brookhaven National Laboratory, which is supported by the U.S. DOE, Divisions of Materials Sciences and Chemical Sciences.

[1] J. B. Goodenough, Prog. Solid State Chem. **5**, 145 (1972), and references therein.
[2] H. Kuwamoto, J. M. Honig, and J. Appel, Phys. Rev. B **22**, 2626 (1980).
[3] D. B. McWhan, T. M. Rice, and J. P. Remeika, Phys. Rev. Lett. **22**, 887 (1969); **23**, 1384 (1969).
[4] J. Ashkenazi and M. Weger, J. Phys. (Paris) **37**, C4-189 (1976).
[5] J. Ashkenazi and T. Chuchem, Philos. Mag. **32**, 763 (1975).
[6] C. Castellani, C. R. Natoli, and J. Ranninger, Phys. Rev. B **18**, 5001 (1978); **18**, 4967 (1978).
[7] C. Castellani, C. R. Natoli, and J. Ranninger, J. Phys. (Paris) **37**, C4-199 (1976).
[8] J. Ashkenazi and M. Weger, Adv. Phys. **22**, 207 (1973).
[9] R. L. Kurtz and V. E. Henrich, Phys. Rev. B **28**, 6699 (1983).
[10] R. L. Kurtz, Ph.D. thesis, Yale University, 1983.
[11] D. B. McWhan, T. M. Rice, and J. P. Remeika, Phys. Rev. Lett. **22**, 887 (1969).
[12] D. B. McWhan, J. P. Remeika, T. M. Rice, W. F. Brinkman, J. P. Maita, and A. Menth, Phys. Rev. Lett. **27**, 941 (1971); D. B. McWhan, J. P. Remeika, S. D. Bader, B. B. Triplett, and N. E. Phillips, Phys. Rev. B **7**, 3079 (1973).
[13] P. Shuker and Y. Yacoby, Phys. Rev. B **14**, 2211 (1976).
[14] P. Hertel and J. Appel, Phys. Rev. B **33**, 2098 (1986).
[15] K. E. Smith and V. E. Henrich, Phys. Rev. B **38**, 5965 (1988).
[16] K. E. Smith and V. E. Henrich, Phys. Rev. B **38**, 9571 (1988).
[17] K. E. Smith and V. E. Henrich, Solid State Commun. **68**, 29 (1988).
[18] S. Shin, S. Suga, M. Taniguchi, M. Fujisawa, H. Kanzaki, A. Fujimori, H. Daimon, Y. Ueda, K. Kosuge, and S. Kachi, Phys. Rev. B **41**, 4993 (1990).

[19]R. L. Kurtz and V. E. Henrich, Phys. Rev. B **25**, 3563 (1982).
[20]K. E. Smith and V. E. Henrich, Surf. Sci. **225**, 47 (1990).
[21]K. E. Smith, Ph.D. thesis, Yale University, 1988.
[22]K. E. Smith and V. E. Henrich, Phys. Rev. B **32**, 5384 (1985).
[23]K. E. Smith, J. L. Mackay, and V. E. Henrich, Phys. Rev. B **35**, 5822 (1987).
[24]M. S. Hegde and S. Vasudevan, Pramana **12**, 151 (1979).
[25]N. F. Mott, *Metal Insulator Transitions* (Taylor and Francis, London, 1974).
[26]J. Hubbard, Proc. R. Soc. London Ser. A **237**, 238 (1963); **281**, 401 (1964).
[27]J. Spalek, A. Datta, and J. M. Honig, Phys. Rev. Lett. **59**, 728 (1987); Phys. Rev. B **33**, 4891 (1986).
[28]G. Sawatzky and D. Post, Phys. Rev. B **20**, 1546 (1979).
[29]D. K. G. deBoer, C. Haas, and G. A. Sawatzky, Phys. Rev. B **29**, 4401 (1984).
[30]B. W. Veal and A. P. Paulikas, Phys. Rev. B **31**, 5399 (1985).
[31]E. Sachar, Phys. Rev. B **31**, 4029 (1985); **34**, 5130 (1986).
[32]S. Doniach and M. Sunjic, J. Phys. C **3**, 285 (1970).
[33]S. Shin, Y. Tezuka, T. Kinoshita, A. Kakizaki, T. Ishii, Y. Ueda, W. Jang, H. Takei, Y. Chiba, and M. Ishigame, Phys. Rev. B **46**, 9224 (1992).
[34]N. Beatham, I. L. Fragala, A. F. Orchard, and G. Thornton, J. Chem. Soc. Faraday Trans. II **76**, 929 (1980).
[35]N. Beatham, A. F. Orchard, and G. Thornton, J. Phys. Chem. Solids **42**, 1051 (1981).
[36]S. Vasudevan, M. S. Hegde, and C. N. R. Rao, Solid State Commun. **27**, 131 (1978).
[37]J. M. Honig, L. L. Van Zandt, R. D. Board, and H. E. Weaver, Phys. Rev. B **6**, 1323 (1972).
[38]C. Blaauw, F. Leenhouts, F. van der Woude, and G. A. Sawatzky, J. Phys. C **8**, 459 (1975).
[39]G. A. Sawatzky and E. Antonides, J. Phys. (Paris) **37**, C4-117 (1976).
[40]V. M. Bermudez, R. T. Williams, J. P. Long, R. K. Reed, and P. H. Klein, Phys. Rev. B **45**, 9266 (1992).